Cancer Management and Research

Dovepress

open access to scientific and medical research

Open Access Full Text Article

ORIGINAL RESEARCH

Long Noncoding RNA *FGD5-AS1* Acts as a Competing Endogenous RNA on microRNA-383 to Enhance the Malignant Characteristics of Esophageal Squamous Cell Carcinoma by Increasing SP1 Expression

This article was published in the following Dove Press journal:
Cancer Management and Research

Jia Gao[1,*]
Ziteng Zhang[2,*]
Hong Su[1]
Ling Zong[2]
Yan Li[1]

[1]Department of Thoracic Surgery, Heze Municipal Hospital, Heze, Shandong 274031, People's Republic of China; [2]Department of Thoracic Surgery, Affiliated Hospital of Jining Medical University, Shandong 272000, People's Republic of China

*These authors contributed equally to this work

Purpose: Previous studies have identified the important roles of a long noncoding RNA called FGD5 antisense RNA 1 (*FGD5-AS1*) in several types of human cancer. Nonetheless, to our knowledge, the expression and functions of FGD5-AS1 in esophageal squamous cell carcinoma (ESCC) have not been clarified. In this study, we aimed to determine the expression status of long noncoding RNA *FGD5-AS1* in ESCC, determine its participation in ESCC progression, and uncover the underlying mechanisms.

Methods: ESCC tissue samples and paired normal adjacent tissues were collected to quantify *FGD5-AS1* expression by reverse-transcription quantitative PCR. The effects of *FGD5-AS1* on ESCC cell proliferation, apoptosis, migration, and invasion in vitro as well as tumor growth in vivo were studied using a Cell Counting Kit-8 assay, flow cytometry, Transwell migration and invasion assays, and an in vivo tumor xenograft experiment.

Results: *FGD5-AS1* was found to be aberrantly upregulated in both ESCC tumors and cell lines compared to the control groups. Increased *FGD5-AS1* expression manifested a close association with tumor size, TNM stage, and lymph node metastasis in patients with ESCC. Overall survival of patients with ESCC was shorter in the *FGD5-AS1* high-expression group than in the *FGD5-AS1* low-expression group. An *FGD5-AS1* knockdown markedly attenuated ESCC cell proliferation, migration, and invasion and promoted apoptosis in vitro as well as slowed tumor growth in vivo. Mechanism investigation revealed that *FGD5-AS1* can increase SP1 expression by sponging microRNA-383 (miR-383), thus functioning as a competing endogenous RNA. An miR-383 knockdown and recovery of SP1 expression attenuated the inhibition of the malignant characteristics of ESCC cells by the *FGD5-AS1* knockdown.

Conclusion: Thus, *FGD5-AS1* enhances the aggressive phenotype of ESCC cells in vitro and in vivo via the miR-383–SP1 axis, which may represent a novel target for ESCC therapy.

Keywords: esophageal squamous cell carcinoma, FGD5 antisense RNA 1, microRNA-383

Introduction

Esophageal cancer, one of the most common malignant tumors, is the eighth most common cancer globally.[1] It is estimated that there will be approximately 455,800 new cases and 400,200 deaths caused by esophageal cancer yearly around the world.[2] Esophageal cancer can be subdivided into two main histological subtypes: esophageal

Correspondence: Yan Li
Department of Thoracic Surgery, Heze Municipal Hospital, No. 2888 Caozhou West Road, Heze, Shandong 274031, People's Republic of China
Email yanli_heze@163.com

squamous cell carcinoma (ESCC) and esophageal adenocarcinoma.[3] ESCC, the main subtype of esophageal cancer, accounts for ~90% of all esophageal cancer cases.[4] Despite remarkable advances in diagnostic and therapeutic techniques in the past decades, clinical outcomes of patients with ESCC remain unsatisfactory, with a dismal 5-year survival rate (less than 20%).[5] Metastasis, recurrence, and resistance to chemo- and radiotherapy are major contributors to the poor prognosis of patients with ESCC.[6] Therefore, detailed investigation of the molecular mechanisms responsible for ESCC initiation and progression is urgently needed to facilitate the identification of novel diagnostic biomarkers and effective therapeutic targets in ESCC.

Noncoding RNAs are a family of transcripts with no protein-coding ability.[7] According to their size and shape, they can be categorized into microRNAs (miRNAs), long noncoding RNAs (lncRNAs), and circular RNAs.[8] LncRNAs are a group of RNA molecules longer than 200 nt; they can modulate gene expression through interactions with miRNAs, thereby attenuating miRNA-driven translational inhibition and/or mRNA degradation.[9] LncRNAs can regulate gene expression via other mechanisms too, including transcriptional modulation, chromatin remodeling, histone modification, and effects on mRNA splicing and stability.[10–12] Aberrant lncRNA expression in ESCC has been widely reported and is implicated in multiple malignant characteristics of ESCC.[13–15] LncRNAs play an important role during ESCC initiation and progression by performing either oncogenic or tumor-suppressive functions.[16–18] These observations collectively uncovered the crucial regulatory role of lncRNAs in the pathogenesis of ESCC, suggesting that lncRNAs might be promising targets for the diagnosis, prognosis, prevention, and treatment of ESCC.

Some studies have identified the crucial involvement of lncRNA *FGD5-AS1* in several types of human cancer.[19–21] Nevertheless, to our knowledge, the expression and functions of *FGD5-AS1* in ESCC have not yet been elucidated. Accordingly, the aim of our study were to determine the expression status of *FGD5-AS1* in ESCC and investigate its regulatory roles in ESCC progression. In addition, we uncovered the mechanisms by which *FGD5-AS1* exerts its oncogenic actions in ESCC cells in vitro and in vivo.

Materials and Methods

Tissue Sample Collection

The study protocol was approved by the Ethics Committee of Heze Municipal Hospital; the study was conducted in accordance with the principles of the Helsinki Declaration. All subjects provided written informed consent prior to their enrollment in this study. All mandatory laboratory health and safety procedures were complied with in the course of conducting all the experimental work reported in this paper. Human ESCC tissue samples and paired normal adjacent tissue samples were obtained from 53 patients with ESCC in Heze Municipal Hospital. None of these patients had received preoperative chemotherapy, radiotherapy, or other anticancer treatments. All tissues were separated, immediately frozen in liquid nitrogen, and stored at −80 °C.

Cell Lines

Human ESCC cell lines, TE-1, KYSE150, KYSE70, and Eca109, were obtained from the Shanghai Institute of the Chinese Academy of Sciences (Shanghai, China). A normal human esophageal epithelial cell line, HET-1A, was acquired from the American Type Culture Collection (Manassas, VA, USA). Dulbecco's modified Eagle's medium (DMEM; Gibco, Grand Island, NY, USA) containing 10% of fetal bovine serum (FBS; Gibco), 100 U/mL penicillin, and 100 μg/mL streptomycin (Gibco) was used for cell culture. Cells were maintained at 37 °C in a humidified incubator supplied with 5% of CO_2.

Transfection

The small interfering RNA (siRNA) specific to *FGD5-AS1* (si-FGD5-AS1) and negative control siRNA (si-NC) were purchased from GenePharma (Shanghai, China). To alter the expression of miR-383, miR-383 agomir (agomir-383) and miR-383 antagomir (antagomir-383) were purchased from RiboBio (Guangzhou, China). The corresponding negative controls (agomir-NC and antagomir-NC) were synthesized by GenePharma (Shanghai, China). To increase the expression of SP1, plasmid pcDNA3.1-SP1 (pc-SP1) was constructed by Sangon Biotech (Shanghai, China); they also supplied the empty pcDNA3.1 vector. The above agomir, antagomir, siRNA, and/or plasmids were transfected into cells using Lipofectamine 2000 (Invitrogen, Carlsbad, CA, USA). The success of transfection was verified via reverse-transcription quantitative polymerase chain reaction (RT-qPCR) or Western blotting.

RT-qPCR

Total RNA was isolated from tissues or cultured cells and quantified, respectively, using the TRIzol Reagent (Invitrogen; Thermo Fisher Scientific, Inc., Waltham, MA, USA) and Nanodrop 2000 (NanoDrop Technologies; Thermo Fisher Scientific, Inc.). To analyze *SP1* mRNA

and *FGD5-AS1* levels, the isolated total RNA was reverse-transcribed using the PrimeScript RT Reagent Kit (Takara Biotechnology Co., Ltd., Dalian, China); subsequently, qPCR was carried out on an Applied Biosystems 7500 Fast Real-Time PCR system (Applied Biosystems; Thermo Fisher Scientific, Inc.) using SYBR Premix Ex Taq™ (Takara Biotechnology Co., Ltd.). Expression levels of *SP1* mRNA and *FGD5-AS1* were normalized to those of the *U6* small nuclear RNA. For miR-383 expression measurement, the miScript Reverse Transcription Kit and miScript SYBR Green PCR Kit (both from Qiagen GmbH, Hilden, Germany) were employed to perform reverse transcription and qPCR, respectively. The *U6* small nuclear RNA served as the endogenous control to normalize miR-383 expression data. All the samples were analyzed in triplicate, and relative expression was calculated using the $2^{-\Delta\Delta Cq}$ method.[22]

Cell Counting Kit-8 (CCK-8) Assay

Preparation of a transfected-cell suspension was conducted 24 h after transfection. Hundred microliters of a cell suspension containing 2×10^3 cells was seeded in each well of 96-well plates. To quantitate cellular proliferation, cells were incubated with 10 μL of the CCK-8 solution (Dojindo Molecular Technologies, Inc., Kumamoto, Japan) at 37 °C for 2 h. The optical density was measured at a wavelength of 450 nm on a microplate reader (Tek, Winooski, VT, USA). The CCK-8 assay was carried out at 0, 24, and 48 h after cell seeding, and a growth curve was plotted accordingly.

Flow Cytometry

Cells transfected with the aforementioned plasmids and/or oligonucleotides were harvested at 48 h post-transfection, washed with pre-cooled phosphate-buffered saline, centrifuged at 2000 rpm for 10 min, and subjected to the quantification of apoptosis using the Annexin V-Fluorescein Isothiocyanate (FITC) Apoptosis Detection Kit (Biolegend, San Diego, CA, USA). In short, the supernatant was removed and the cells were resuspended in 100 μL of 1× binding buffer; then, the cells were labeled with 5 μL of annexin V-FITC and 10 μL of a propidium iodide solution. After incubation for 15 min in the dark, the rate of apoptosis was analyzed on a flow cytometer (BD Biosciences, Franklin Lakes, NJ, USA).

Transwell Migration and Invasion Assays

Transfected cells that had undergone 48 h of incubation were trypsinized and resuspended in FBS-free DMEM. The concentration of the cell suspension was adjusted to 10^5 cells/mL. Transwell chambers (8.0 μm pore size; Corning Inc., Corning, NY, USA) precoated with Matrigel (BD Biosciences) were used for the Transwell invasion assay, whereas the migration assay was carried out in Transwell chambers that were not coated with Matrigel. For each assay, 200 μL of a cell suspension was added into the upper compartment of the Transwell chambers and 600 μL of DMEM containing 20% of FBS (as a chemoattract) was added into the bottom compartments. After 24 h cultivation at 37 °C, nonmigratory and noninvasive cells were carefully wiped off with a cotton swab. The migratory or invasive cells were fixed with 95% ethanol and stained with 0.5% crystal violet. The images of stained cells were captured to determine the number of migratory or invasive cells using an inverted microscope (Olympus, Tokyo, Japan).

In vivo Tumor Xenograft Experiment

The animal experimental protocols were approved by the Animal Care and Use Committee of Heze Municipal Hospital. All experimental steps were in accordance with the Animal Protection Law of the People's Republic of China-2009 for experimental animals. BALB/c nude mice (4–6 weeks old) were purchased from Beijing HFK Bioscience (Beijing, China) and maintained under specific pathogen-free conditions.

Plasmids expressing *FGD5-AS1*-targeting short hairpin RNA (pLKO.1-sh-FGD5-AS1) or negative control short hairpin RNA (pLKO.1-sh-NC) were acquired from GenePharma. To establish stable knockdown cell lines, either pLKO.1-sh-FGD5-AS1 or pLKO.1-sh-NC was introduced into cells using Lipofectamine 2000. TE-1 cells were transfected with a lentivirus containing either pLKO.1-sh-FGD5-AS1 or pLKO.1-sh-NC and were selected with 2 μg/mL puromycin. In total, 5×10^6 TE-1 cells stably transfected with either sh-FGD5-AS1 or sh-NC were subcutaneously injected into a flank of each nude mouse. The size (width and length) of the resultant tumor xenografts in groups "sh-FGD5-AS1" and "sh-NC" was measured starting on day 10 for 1 month; their volume was calculated using the following formula: $0.5 \times \text{length} \times \text{width}^2$. All mice were euthanized at 30 days after the cell injection, and the tumor xenografts were excised and analyzed by RT-qPCR and Western blotting.

Bioinformatic Prediction

The starBase 3.0 software (http://starbase.sysu.edu.cn/) was utilized to predict *FGD5-AS1*–miRNA interaction. Additionally, putative targets of miR-383 were predicted in three bioinformatic databases: TargetScan (http://www.targetscan.org/), miRDB (http://mirdb.org/), and starBase 3.0.

An RNA Immunoprecipitation (RIP) Assay

The Magna RIP RNA-Binding Protein Immunoprecipitation Kit (Millipore, Bedford, MA, USA) was used for the RIP assay, to assess the interaction between *FGD5-AS1* and miR-383 in ESCC cells. The cells were lysed in RNA immunoprecipitation buffer. The magnetic beads conjugated with either a human anti-AGO2 antibody (Millipore) or IgG control (Millipore) were then incubated with the whole-cell extracts. After digestion of the protein using proteinase K, the immunoprecipitated RNA was analyzed via RT-qPCR.

A Luciferase Reporter Assay

The fragment of the 3′-untranslated region (UTR) of *SP1* containing either the wild-type (wt) miR-383-binding site or the mutant (mut) site was amplified by GenePharma and inserted into the pmirGLO Dual-Luciferase reporter vector (Promega, Madison, WI, USA), thereby resulting in reporter vectors SP1-wt and SP1-mut. To evaluate the direct interaction between *FGD5-AS1* and miR-383, reporter plasmids FGD5-AS1-wt and FGD5-AS1-mut were chemically synthesized via similar experimental steps. For the reporter assay, a luciferase reporter vector was cotransfected with either agomir-383 or agomir-NC into ESCC cells that were seeded in 24-well plates. After 48 h incubation, the transfected cells were collected and the luciferase activity was evaluated in the Dual-Luciferase Reporter Assay (Promega). The level of *Renilla* luciferase activity served as the control for the normalization of firefly luciferase activity.

Western Blotting

The extraction of total protein was carried out using RIPA lysis buffer (Beyotime Biotechnology, Shanghai, China). Total protein in the cell lysates was quantitated by the bicinchoninic acid (BCA) assay (Beyotime Biotechnology). Equal amounts of protein were resolved by sodium dodecyl sulfate 10% polyacrylamide gel electrophoresis and then transferred to polyvinylidene difluoride membranes. Next, 5% defatted milk powder dissolved in Tris-buffered saline (TBS) containing 0.1% of Tween 20 (TBS-T) was used to blocking the membranes at room temperature for 2 h. After incubation with primary antibodies overnight at 4 °C, the membranes were extensively washed with TBS-T, incubated with a horseradish peroxidase-conjugated secondary antibody (1:5000 dilution in TBS-T; cat. No. sc-516102; Santa Cruz Biotechnology, Inc., Dallas, TX, USA) at room temperature for 1 h, and finally subjected to protein signal detection via enhanced chemiluminescence using the ECL Kit (Pierce; Thermo Fisher Scientific, Inc.). An anti-SP1 antibody (1:1000; cat. No. sc-17824) (primary antibody) was purchased from Santa Cruz Biotechnology, and an anti-GAPDH antibody (1:1000; cat. No. sc-6977, Santa Cruz Biotechnology) was employed to set up a loading control.

Statistical Analysis

All results are presented as the means ± standard error from experiments repeated at least three times. Correlations between *FGD5-AS1* expression and clinicopathological parameters of patients with ESCC were analyzed via the $\chi 2$ test. One-way analysis of variance (ANOVA) followed by the Bonferroni–Dunn test was conducted to evaluate the differences among multiple groups. A comparison between two groups was made using Student's *t*-test. The Kaplan–Meier method and logrank test were used to examine the correlation between overall survival and *FGD5-AS1* expression among patients with ESCC. Spearman correlation analysis was performed to study the correlation between *FGD5-AS1* and miR-383 expression levels in ESCC tissue samples. All statistical analyses were conducted using SPSS 19.0 software (IBM SPSS, Armonk, NY, USA), with a P value less than 0.05 indicating statistical significance.

Results

FGD5-AS1 Is Overexpressed in ESCC Tumors and Cell Lines

To gain insight into the expression pattern of *FGD5-AS1* in ESCC, its levels in 53 pairs of ESCC tissue samples and normal adjacent tissues were determined via RT-qPCR. The results revealed that the expression of *FGD5-AS1* was higher in ESCC tissue samples than in the normal adjacent tissues (Figure 1A, $P < 0.05$).

The expression of *FGD5-AS1* was also tested in four ESCC cell lines (TE-1, KYSE150, KYSE70, and Eca109) and in a normal human esophageal epithelial cell line: HET-1A. The results of RT-qPCR indicated that *FGD5-AS1* was upregulated in all four ESCC cell lines in comparison with HET-1A cells (Figure 1B, $P < 0.05$). As *FGD5-AS1* was more strongly expressed in TE-1 and Eca109 cells compared

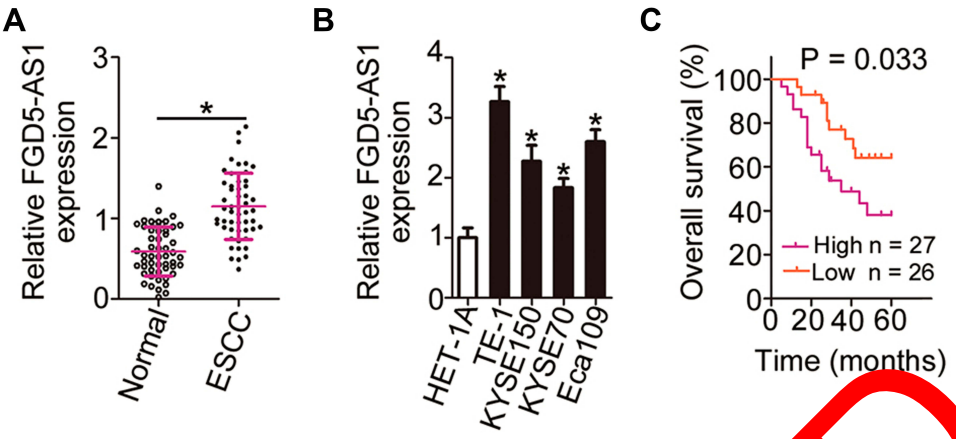

Figure 1 2*FGD5-AS1* is highly expressed in ESCC. (**A**) Expression of *FGD5-AS1* was analyzed using RT-qPCR in 53 pairs of ESCC tissue samples and normal adjacent tissues. *P < 0.05 vs normal adjacent tissues. (**B**) RT-qPCR was carried out to measure *FGD5-AS1* expression in four ESCC cell lines (TE-1, KYSE150, KYSE70, and Eca109) and in a normal human esophageal epithelial cell line, HET-1A. *P < 0.05 vs HET-1A cells. (**C**) The Kaplan–Meier method and logrank test were applied to examine the association between *FGD5-AS1* expression and overall survival among patients with ESCC. P = 0.033.

to KYSE150 and KYSE70 cells, subsequent functional assays were performed on the first two cell lines.

To address the clinical value of *FGD5-AS1* in ESCC, the ESCC tissue samples were classified into either the *FGD5-AS1* high-expression group or *FGD5-AS1* low-expression group on the basis of the *FGD5-AS1* median level among the ESCC tissue samples. Higher expression of *FGD5-AS1* was found to correlate with tumor size (P = 0.024), TNM stage (P = 0.027), and lymph node metastasis (P = 0.021) among the patients with ESCC (Table 1). In addition, patients in the *FGD5-AS1* high-expression group showed shorter overall survival compared to the patients in the *FGD5-AS1* low-expression group (Figure 1C, P = 0.033).

The *FGD5-AS1* Knockdown Inhibits the Growth and Metastasis of ESCC Cells

To directly investigate whether *FGD5-AS1* is implicated in the malignancy of ESCC, si-FGD5-AS1 was transfected into TE-1 and Eca109 cells to reduce *FGD5-AS1* expression in the two cell lines. RT-qPCR analysis of TE-1 and Eca109 cells verified the success of the *FGD5-AS1* knockdown by si-FGD5-AS1 transfection (Figure 2A, P < 0.05). To assess the influence of the *FGD5-AS1* knockdown on the proliferation and apoptosis of ESCC cells, the CCK-8 assay and flow-cytometric analysis were performed on the *FGD5-AS1*–deficient TE-1 and Eca109 cells. As indicated in Figure 2B and C, the knockdown of *FGD5-AS1* obviously decreased proliferation (P < 0.05) and enhanced the apoptosis (P < 0.05) of TE-1 and Eca109 cells. Furthermore, Transwell migration and invasion assays were conducted to determine cellular migration and invasion. A significant decrease in the migratory (Figure 2D, P < 0.05) and invasive (Figure 2E, P < 0.05) abilities of TE-1 and Eca109 cells was observed upon transfection with si-FGD5-AS1. In short, *FGD5-AS1* was found to serve as an oncogenic lncRNA in ESCC cells in vitro.

Table 1 The Correlation Between FGD5-AS1 Expression and the Clinicopathological Parameters in Patients with Esophageal Squamous Cell Carcinoma

Parameters	FGD5-AS1 Expression		P-value
	High	Low	
Age (years)			0.347
< 60	10	12	
≥ 60	17	14	
Gender			0.398
Male	15	18	
Female	12	8	
Tumor size (cm)			0.024*
< 5	12	20	
≥ 5	15	6	
Differentiation status			0.583
Well and moderately	14	16	
Poor	13	10	
TNM stage			0.027*
I–II	11	19	
III	16	7	
Lymph node metastasis			0.021*
Negative	13	21	
Positive	14	5	

Note: *P<0.05.

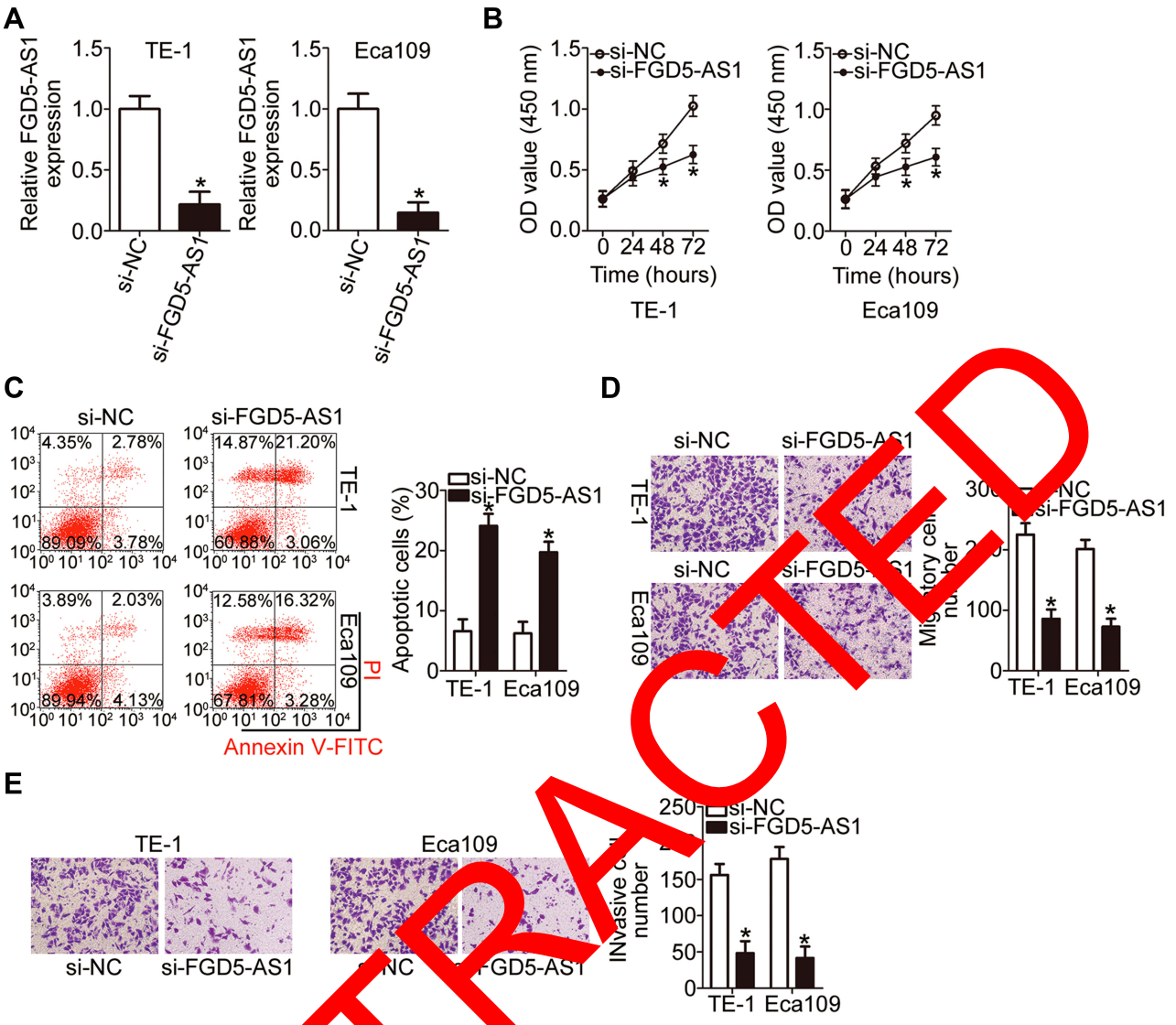

Figure 2 The *FGD5-AS1* knockdown restricts the prolifer[illegible]n, migration, and invasiveness and induces apoptosis of TE-1 and Eca109 cells. (**A**) Si-FGD5-AS1 was used to knock down endogenous *FGD5-AS1* in [illegible]-1 and Eca109 cell[illegible]d this knockdown was verified via RT-qPCR. *P < 0.05 vs the si-NC group. (**B, C**) The proliferation and apoptosis of *FGD5-AS1*-deficient TE[illegible] and Eca109 cells were ev[illegible]ated by the CCK-8 assay and flow cytometry. *P < 0.05 compared with group "si-NC." (**D, E**) Transwell migration and invasion assays w[illegible] conducte[illegible] assess the migration and invasiveness of the *FGD5-AS1* knockdown TE-1 and Eca109 cells. *P < 0.05 vs group si-NC.

FGD5-AS1 Interacts with miR-383 and Sponges miR-[illegible] in ESCC Cells

To illustrate the mechanism by which *FGD5-AS1* enhances the malignant characteristics of ESCC cells, a potential target miRNA of *FGD5-AS1* was predicted using StarBase 3.0. The bioinformatic prediction indicated that *FGD5-AS1* (Figure 3A) carries a putative binding site for miR-383. The latter was chosen for experimental verification because this miRNA has frequently been implicated in multiple types of human tumors.[23–27] The luciferase reporter assay was performed to test whether miR-383 can directly bind to *FGD5-AS1* in ESCC cells. Either reporter plasmid FGD5-AS1-wt or FGD5-AS1-mut was transfected into TE-1 and Eca109 cells along with either agomir-383 or agomir-NC. First, the transfection efficiency was verified in these TE-1 and Eca109 cells through quantitation of miR-383 by RT-qPCR (Figure 3B, $P < 0.05$). The cotransfection of FGD5-AS1-wt and agomir-383 notably decreased the luciferase activity ($P < 0.05$); however, no change in the luciferase activity of FGD5-AS1-mut-transfected TE-1 and Eca109 cells was seen in the presence of agomir-383 (Figure 3C). Furthermore, the RIP assay indicated that miR-383 was substantially enriched in the presence of *FGD5-AS1* in both TE-1 and Eca109 cells (Figure 3D, $P < 0.05$).

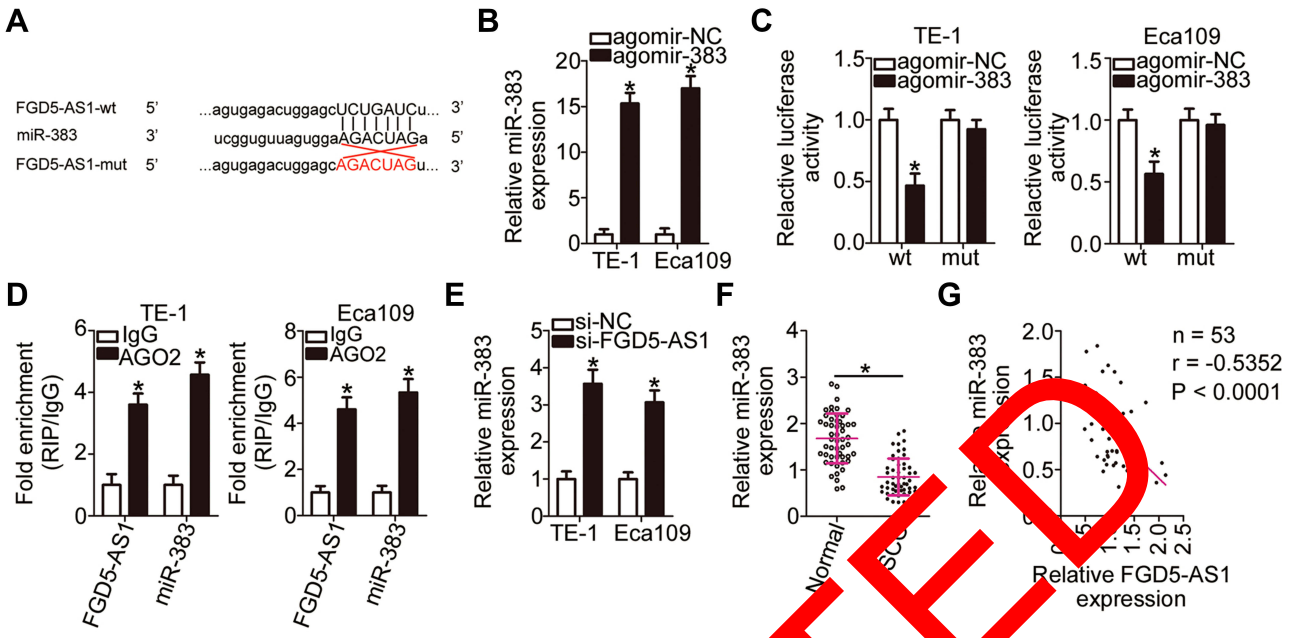

Figure 3 MiR-383 is a target of *FGD5-AS1* in ESCC cells. (**A**) The schematic diagram of the wild-type (wt) and mutated (mt) miR-383–binding sequences within *FGD5-AS1*. (**B**) Agomir-383 was introduced into TE-1 and Eca109 cells to increase miR-383 levels. *P < 0.05 vs group "agomir-NC." (**C**) The luciferase reporter vectors harboring either the wild-type or mutated miR-383–binding site were synthesized and cotransfected with either miR-383 or agomir-NC into TE-1 and Eca109 cells. Luciferase activity was measured after 48 h of incubation. *P < 0.05 compared with the agomir-NC group. (**D**) The RIP assay was carried out, and expression of miR-383 and *FGD5-AS1* was measured in the immunoprecipitate of either the anti-AGO2 antibody or IgG control from the lysates of TE-1 and Eca109 cells. *P < 0.05 vs the IgG group. (**E**) TE-1 and Eca109 cells were transfected with either si-FGD5-AS1 or si-NC. At 48 h post-transfection, total RNA was extracted and subjected to RT-qPCR analysis for the measurement of miR-383 expression. *P < 0.05 vs group si-NC. (**F**) MiR-383 expression in 53 pairs of ESCC tissue samples and normal adjacent tissues was tested via RT-qPCR. *P < 0.05 compared with normal adjacent tissues. (**G**) The correlation between miR-383 and *FGD5-AS1* expression levels among the 53 ESCC tissue samples was assessed by Spearman correlation analysis. r = –0.5352, P < 0.0001.

We next determined whether miR-383 could be sponged by *FGD5-AS1* in ESCC cells. RT-qPCR analysis was carried out to measure miR-383 expression in TE-1 and Eca109 cells after transfection with either si-FGD5-AS1 or si-NC; the results revealed that the knockdown of *FGD5-AS1* substantially increased miR-383 expression (Figure 3E, P < 0.05). Furthermore, the expression of miR-383 was measured by RT-qPCR in the 53 pairs of ESCC tissue samples and normal adjacent tissue samples. The data showed that miR-383 was significantly underexpressed in the ESCC tissue samples compared to the normal adjacent tissues (Figure 3F, P < 0.05), the by manifesting an inverse correlation with *FGD5-AS1* expression in the ESCC tissue samples (Figure 3G; r = –0.5352, P < 0.0001). These results collectively identified miR-383 as a target of *FGD5-AS1* in ESCC cells.

FGD5-AS1 Functions as a Competing Endogenous RNA (ceRNA) for miR-383 and Thereby Increases SP1 Expression

According to the three bioinformatic databases, the seed region of miR-383 contains a sequence complementary to a site in the 3′-UTR of *SP1* mRNA (Figure 4A). The luciferase reporter assay was conducted to confirm the binding of miR-383 to the 3′-UTR of *SP1* mRNA in ESCC cells. The luciferase activity of reporter plasmid SP1-wt was dramatically lower in miR-383-overexpressing TE-1 and Eca109 cells (P < 0.05), whereas the mutation of the miR-383-binding site abrogated the negative impact of miR-383 upregulation on the luciferase activity (Figure 4B). To test whether the expression of SP1 was reduced by miR-383, agomir-383 was utilized to increase the miR-383 level; then, we carried out RT-qPCR and Western blotting to respectively measure SP1 mRNA and protein amounts. The mRNA (Figure 4C, P < 0.05) and protein (Figure 4D, P < 0.05) levels of SP1 were lower in TE-1 and Eca109 cells after transfection with agomir-383. In addition, *SP1* mRNA expression was higher in ESCC tissue samples than in normal adjacent tissues (Figure 4E, P < 0.05). Spearman correlation analysis proved an inverse correlation between *SP1* mRNA and miR-383 expression levels among the 53 ESCC tissue samples (Figure 4F; r = –0.5854, P < 0.0001). These results provided sufficient evidence that *SP1* is a direct target gene of miR-383 in ESCC cells.

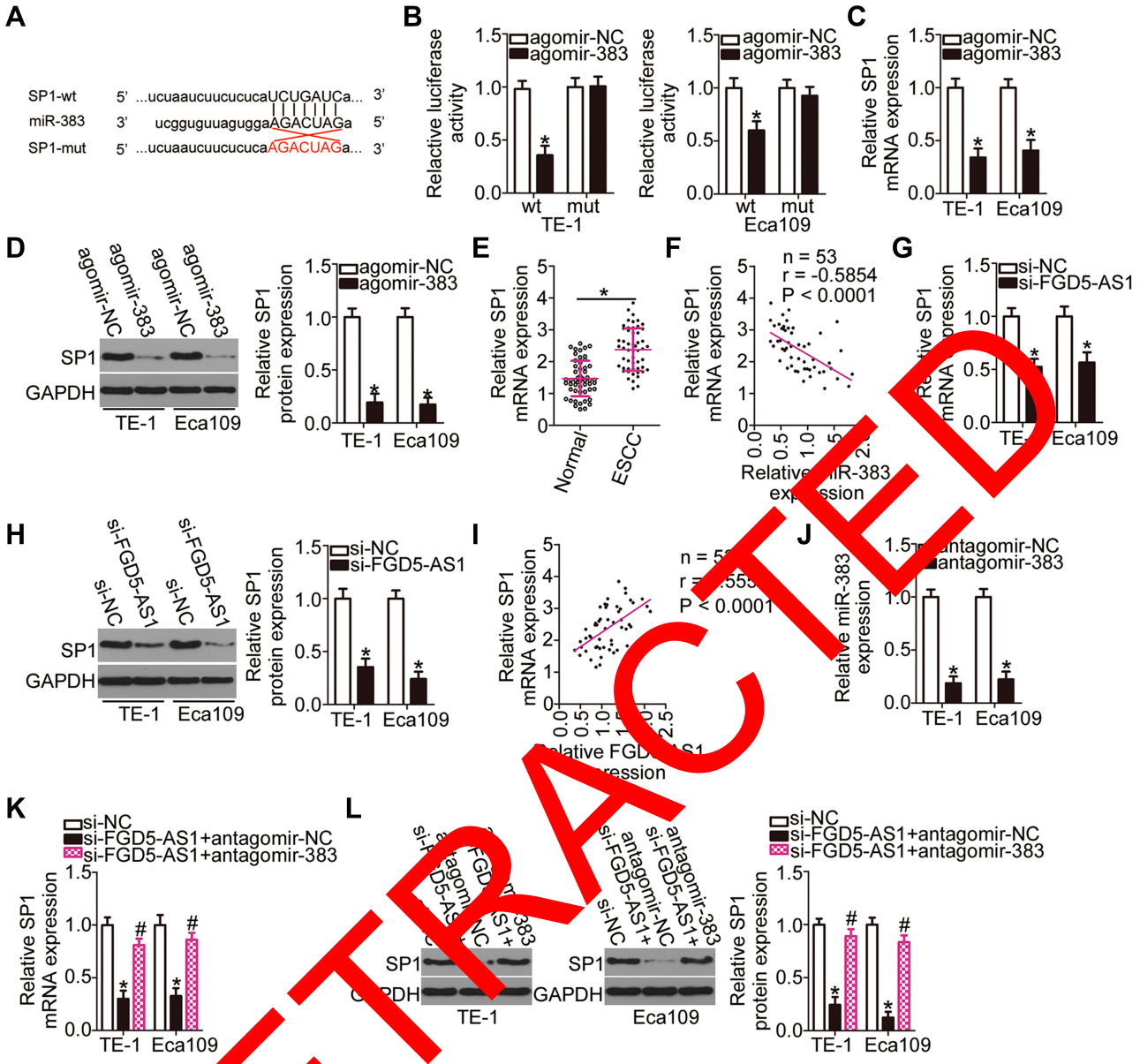

Figure 4 *FGD5-AS1* functions as ceRNA for miR-383 and thereby enhances SP1 expression (**A**) The predicted binding site for miR-383 in the 3′-UTR of *SP1* mRNA. The mutated binding sequence is depicted. (**B**) The luciferase activity in TE-1 and Eca109 cells cotransfected with either SP1-wt or SP1-mut and either agomir-383 or agomir-NC was detected in the luciferase reporter assay. *P < 0.05 vs group "agomir-NC." (**C, D**) RT-qPCR and Western blotting were carried out to quantitate SP1 mRNA and protein expression in TE-1 and Eca109 cells following agomir-383 or agomir-NC transfection. *P < 0.05 vs the agomir-NC group. (**E**) Analysis of *SP1* mRNA expression in the 53 pairs of ESCC tissue samples and normal adjacent tissues was conducted by RT-qPCR. *P < 0.05 vs normal adjacent tissues. (**F**) The inverse correlation between *SP1* mRNA and miR-383 expression among the 53 ESCC tissue samples was identified in Spearman correlation analysis. r = –0.5854, P < 0.0001. (**G, H**) The mRNA and protein expression of SP1 in *FGD5-AS1*-deficient TE-1 and Eca109 cells was quantified via RT-qPCR and Western blotting, respectively. *P < 0.05 compared with group si-NC. (**I**) The correlation between *FGD5-AS1* and SP1 mRNA expressions among the 53 ESCC tissue samples was assessed by Spearman correlation analysis. r = 0.5558, P < 0.0001. (**J**) Examination of miR-383 expression by RT-qPCR in TE-1 and Eca109 cells that were transfected with either antagomir-NC or antagomir-383. *P < 0.05 vs the antagomir-NC group. (**K, L**) FGD5-AS1 in combination with either antagomir-NC or antagomir-383 was transfected into TE-1 and Eca109 cells. After the transfection, mRNA and protein levels of SP1 were respectively analyzed through RT-qPCR and Western blotting. *P < 0.05 vs the si-NC group, #P < 0.05 vs group si-FGD5-AS1 +antagomir-NC.

As *FGD5-AS1* and *SP1* mRNA share the same miR-383-binding site, we hypothesized that *FGD5-AS1* may regulate SP1 expression by functioning as a ceRNA for miR-383 in ESCC cells. RT-qPCR and Western blotting were carried out to respectively measure SP1 mRNA and protein expression in *FGD5-AS1*-deficient TE-1 and Eca109 cells. The *FGD5-AS1* knockdown reduced the expression of SP1 in TE-1 and Eca109 cells at the mRNA (Figure 4G, P < 0.05) and protein levels (Figure 4H, P < 0.05). Spearman correlation analysis was

also performed to evaluate the expression correlation between *FGD5-AS1* and SP1 mRNA in ESCC tissue samples. As displayed in Figure 4I, expression of *FGD5-AS1* was positively correlated with that of SP1 mRNA expression in the 53 ESCC tissues ($r = 0.5558$, $P < 0.0001$). Rescue experiments were conducted to determine whether *FGD5-AS1* controls SP1 expression in ESCC cells through interactions with miR-383. Antagomir-383 transfection markedly reduced the expression of miR-383 in TE-1 and Eca109 cells as evidenced by RT-qPCR (Figure 4J, $P < 0.05$). Si-FGD5-AS1 together with either antagomir-383 or antagomir-NC was transfected into TE-1 and Eca109 cells and then RT-qPCR and Western blotting were performed. The effects of the *FGD5-AS1* knockdown on SP1 mRNA (Figure 4K, $P < 0.05$) and protein amounts (Figure 4L, $P < 0.05$) were reversed by antagomir-383. Thus, *FGD5-AS1* may positively regulate SP1 expression in ESCC cells by sponging miR-383.

The *FGD5-AS1* Knockdown Inhibits the Malignancy of ESCC Cells Through the miR-383–SP1 Axis

Rescue experiments were conducted to test whether the oncogenic activities of *FGD5-AS1* in ESCC cells are dependent on the miR-383–SP1 axis. To this end, TE-1 and Eca109 cells were cotransfected with si-FGD5-AS1 and either antagomir-383 or antagomir-NC and cell proliferation, apoptosis, migration, and invasion were studied in the cotransfected cells. The inhibition of proliferation (Figure 5A, $P < 0.05$), promotion of apoptosis (Figure 5B, $P < 0.05$), and suppression of the migratory (Figure 5C, $P < 0.05$) and invasive (Figure 5D, $P < 0.05$) capabilities of *FGD5-AS1*-deficient TE-1 and Eca109 cells were greatly reversed upon antagomir-383 cotransfection.

Similarly, we restored SP1 expression in the *FGD5-AS1*-deficient TE-1 and Eca109 cells via cotransfection with the SP1-overexpressing plasmid (pc-SP1) and carried out the CCK-8 assay, flow-cytometric analysis, and Transwell migration and invasion assays. First, the efficiency of pc-SP1 transfection was verified by Western blotting (Figure 6A, $P < 0.05$). The reduction in *FGD5-AS1* expression inhibited TE-1 and Eca109 cell proliferation (Figure 6B, $P < 0.05$) and promoted apoptosis (Figure 6C, $P < 0.05$); these alterations were notably attenuated by the recovery of SP1 expression. In addition, the effects of the *FGD5-AS1* knockdown on the migration (Figure 6D, $P < 0.05$) and invasiveness (Figure 6E, $P < 0.05$) of TE-1 and Eca109 cells were weakened by the reintroduction of SP1. Therefore, these results meant that the miR-383–SP1 axis mediates the stimulatory influence of *FGD5-AS1* on the malignant behavior of ESCC cells.

The *FGD5-AS1* Knockdown Reduces Tumor Growth of ESCC Cells in vivo

In vivo tumor xenograft experiments were conducted to examine the impact of *FGD5-AS1* on the tumor growth of ESCC cells in vivo. TE-1 cells stably transfected with either sh-FGD5-AS1 or sh-NC were subcutaneously injected into the flanks of nude mice. The volume (Figure 7A and B, $P < 0.05$) and weight (Figure 7C, $P < 0.05$) of the resultant tumor xenografts in the sh-FGD5-AS1 group were much smaller than those in the sh-NC group. The tumor xenografts were resected at the end of this experiment and subjected to RT-qPCR and Western blotting analyses. The tumor xenografts derived from sh-FGD5-AS1–transfected TE-1 cells manifested decreased *FGD5-AS1* (Figure 7D, $P < 0.05$), increased miR-383 (Figure 7E, $P < 0.05$), and downregulated SP1 protein (Figure 7F, $P < 0.05$) levels in comparison with the sh-NC group. In brief, the *FGD5-AS1* knockdown targeted the miR-383–SP1 axis, thereby retarding the tumor growth of ESCC cells in vivo.

Discussion

The complicated nature of the pathogenesis of ESCC has seriously hampered relevant clinical research and therapy.[28,29] In the past few years, several lines of evidence revealed that lncRNAs are aberrantly expressed in ESCC and that this aberration is deeply implicated in the aggressive phenotype of ESCC cells.[30–32] Therefore, lncRNAs have potential as effective diagnostic and therapeutic targets in ESCC. Although numerous lncRNAs have been validated to be closely linked to ESCC progression, only a small minority of lncRNAs has been studied well, leaving multiple crucial issues to be resolved. Here, we attempted to explore the expression characteristics of *FGD5-AS1* in ESCC and determine whether *FGD5-AS1* can regulate the malignancy of ESCC in vitro and in vivo.

FGD5-AS1 is overexpressed in colorectal cancer.[19] Depletion of *FGD5-AS1* inhibits colorectal cancer cell proliferation, migration, and invasion and increases apoptosis in vitro.[19] *FGD5-AS1* also plays an important part in small cell lung cancer[20] and clear cell kidney carcinoma.[21] Nevertheless, the expression and roles of *FGD5-AS1* in ESCC have not yet been clarified. Herein, we performed RT-qPCR analysis to determine *FGD5-AS1* expression in ESCC and demonstrated that *FGD5-AS1* is upregulated in ESCC

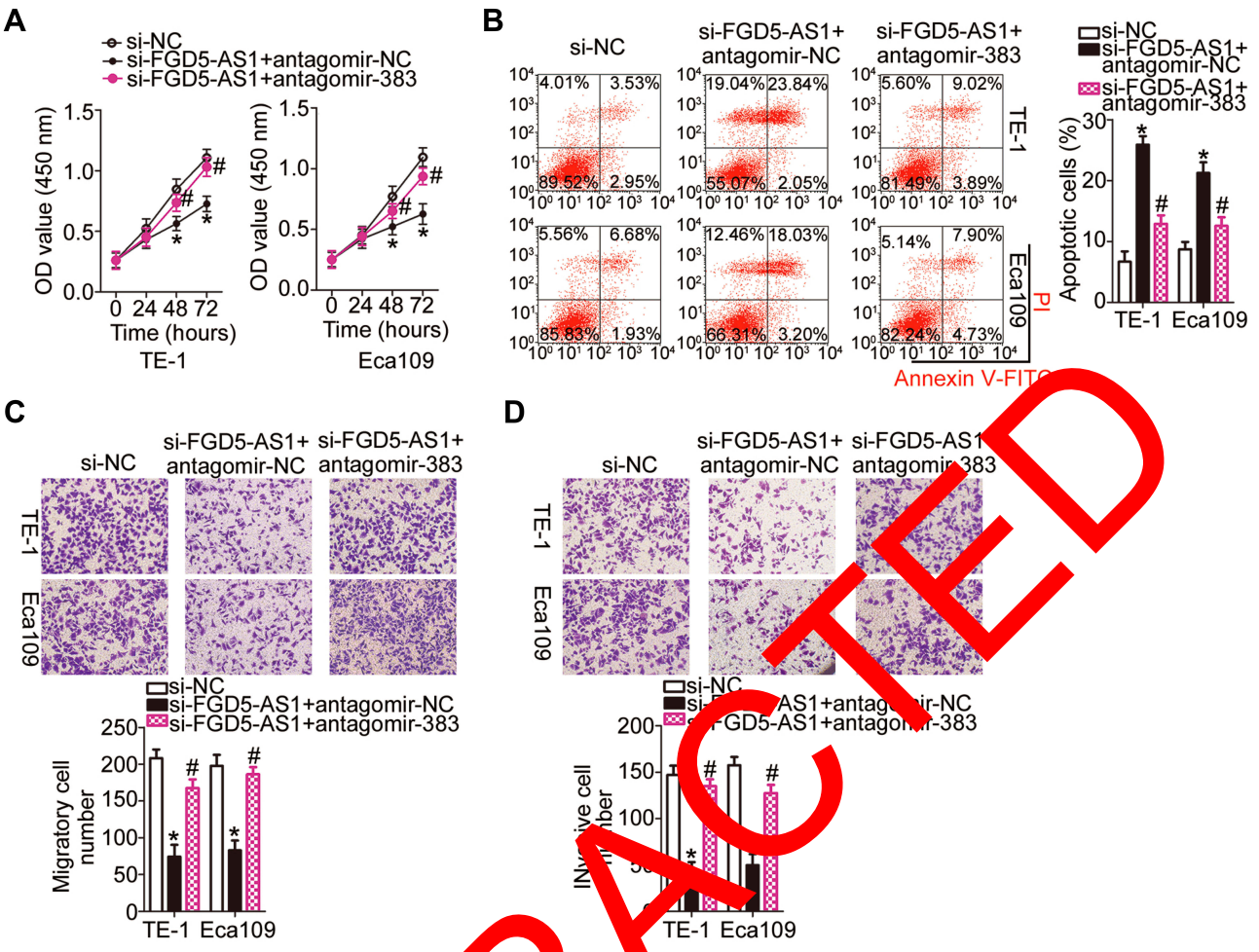

Figure 5 The miR-383 knockdown can reverse the suppressive effects of the *FGD5-AS1* knockdown on the malignant characteristics of TE-1 and Eca109 cells. (**A, B**) Si-FGD5-AS1 was cotransfected with either antagomir-383 or antagomir-NC into TE-1 and Eca109 cells. The proliferation and apoptosis were studied by the CCK-8 assay and flow cytometry. *P < 0.05 vs the si-NC group. #P < 0.05 vs group si-FGD5-AS1+antagomir-NC. (**C, D**) Transwell migration and invasion assays were performed to examine the migratory and invasive capabilities of TE-1 and Eca109 cells that were treated as described above. *P < 0.05 vs group si-NC. #P < 0.05 vs group si-FGD5-AS1+antagomir-NC.

tumors and cell lines. High *FGD5-AS1* expression showed a significant correlation with tumor size, TNM stage, lymph node metastasis, and shorter overall survival among patients with ESCC. In terms of function, *FGD5-AS1* knockdown led to an obvious reduction in cell proliferation, migration, and invasion as well as induction of apoptosis. Furthermore, *FGD5-AS1* silencing retarded the tumor growth of ESCC cells in vivo. However, in this study, we did not perform rescue assays in tumor growth experiment to validate the in vitro mechanistic findings. It was a limitation of our study, and we will resolve it in the near future.

LncRNAs act as ceRNAs competitively interacting with miRNAs and thus upregulate specific mRNAs.[33] As for the mechanism, *FGD5-AS1* can increase CDCA7 expression by sponging miR-302e and thereby raises the malignancy of colorectal cancer.[19] To gain a complete understanding of the oncogenic activities of *FGD5-AS1* in ESCC, a series of experiments was conducted in this study to elucidate the mechanism of action. First, a bioinformatic prediction indicated that *FGD5-AS1* contains a putative miR-383-binding site. Second, luciferase reporter and RIP assays suggested that miR-383 can directly interact with *FGD5-AS1* in ESCC cells. Third, the knockdown of *FGD5-AS1* increased the expression of miR-383 in ESCC cells. Fourth, miR-383 turned out to be only weakly expressed in ESCC tissue samples, manifesting an inverse correlation with *FGD5-AS1* expression. Fifth, the knockdown of *FGD5-AS1* decreased SP1 expression in ESCC cells at both the mRNA and protein levels and the positive influence of *FGD5-AS1* on SP1 expression was demonstrated to be mediated by the sponging of miR-383. Finally, the miR-383 knockdown and SP1 overexpression greatly attenuated the inhibitory influence of the *FGD5-AS1* knockdown on the malignancy of ESCC cells. As a consequence, our study

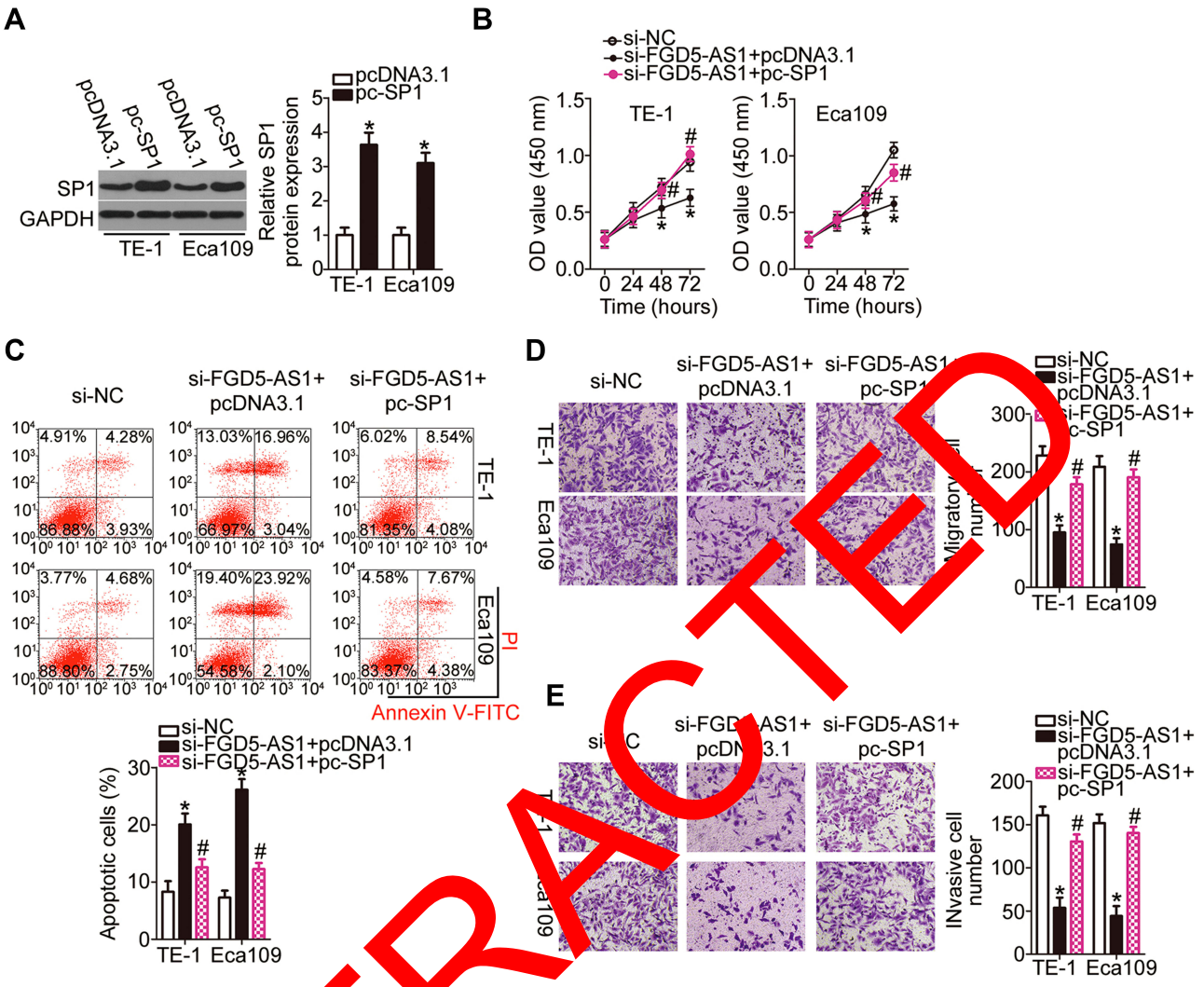

Figure 6 SP1 reintroduction can abrogate the effects of the *FGD5-AS1* knockdown on the malignant characteristics of TE-1 and Eca109 cells. (**A**) Western blotting was conducted to determine the efficiency of pc-SP1 transfection in TE-1 and Eca109 cells. $^{*}P < 0.05$ compared with the empty pcDNA3.1 vector group. (**B**–**E**) The proliferation, apoptosis, migration, and invasiveness of TE-1 and Eca109 cells cotransfected with si-FGD5-AS1 and either plasmid ps-SP1 or the empty pcDNA3.1 vector were respectively investigated by the CCK-8 assay, flow-cytometric analysis, and Transwell migration and invasion assays. $^{*}P < 0.05$ vs the si-NC group. $^{\#}P < 0.05$ vs group si-FGD5-AS1+pcDNA3.1.

proved that *FGD5-AS1* performs a tumor-promoting function in ESCC cells by acting as a ceRNA on miR-383 and thereby upregulating SP1.

MiR-383 exerts important actions on the progression of various human cancers. For example, miR-383 is underexpressed in gastric cancer,[23,24] thyroid cancer,[25] hepatocellular carcinoma,[25] and ovarian cancer.[26] Functionally, miR-383 serves as a tumor-suppressive miRNA in the above-mentioned human cancer types. On the contrary, miR-383 is upregulated in cholangiocarcinoma[27] and stimulates cancer progression. To our knowledge, this study is the first to show that miR-383 expression is low in ESCC and that miR-383 directly targets *SP1* mRNA in ESCC cells.

SP1, located in chromosomal region 12q13.1, encodes a sequence-specific DNA-binding protein.[34] SP1 is capable of either stimulating or inhibiting the activity of gene promoters by directly interacting with GC/GT-rich promoter elements via its C(2)H(2)-type zinc fingers in C-terminal domains.[35] The dysregulation of SP1 contributes to cancer initiation and progression by affecting a wide variety of biological behaviors.[36–38] SP1 is also reported to be highly expressed in ESCC, and the upregulation of SP1 is closely related to the malignant progression of ESCC.[39–41] Our study indicates that the knockdown of *FGD5-AS1* reduces miR-383 sponging, thus reducing SP1 expression in ESCC, thereby diminishing the malignancy of ESCC cells in vitro and in vivo. These results point to an ESCC pathogenesis-related regulatory network, which is composed of *FGD5-AS1*, miR-383, and SP1. This knowledge about the *FGD5-AS1*–miR-

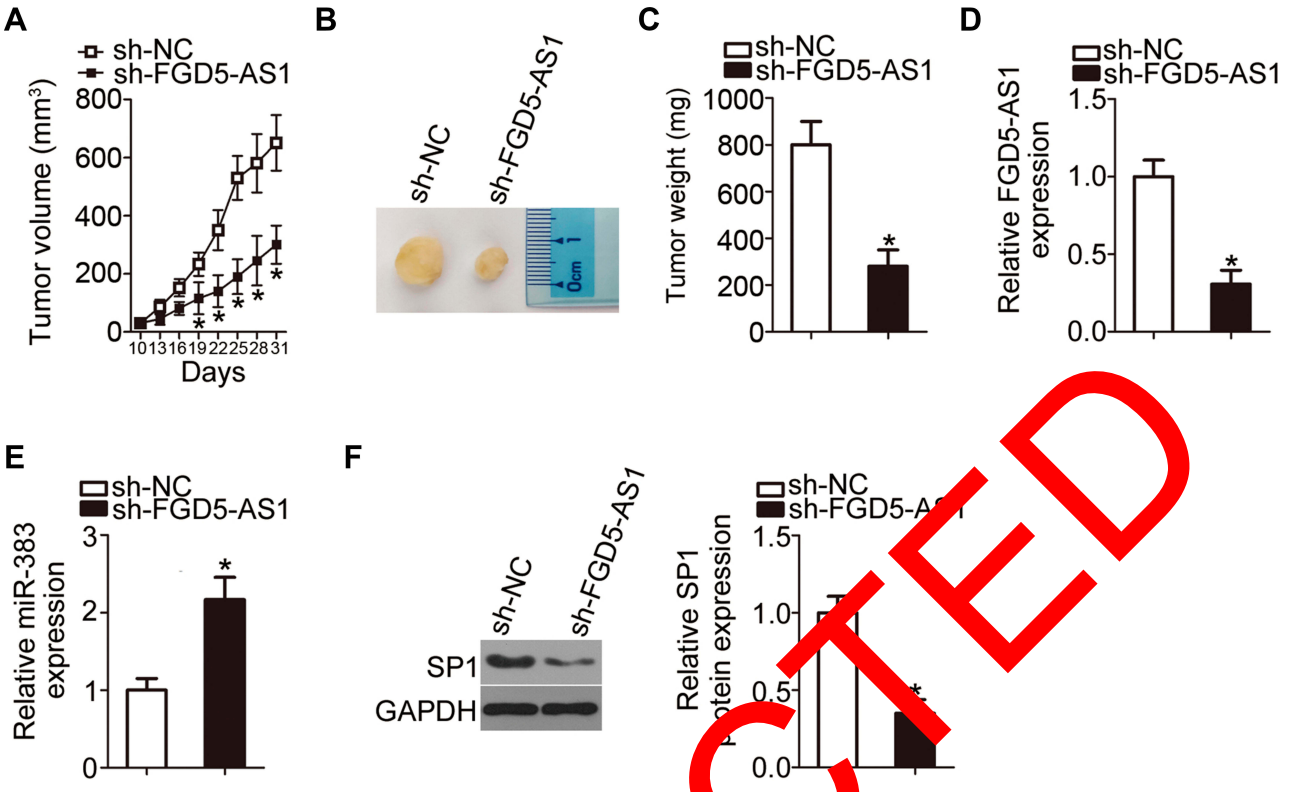

Figure 7 The knockdown of *FGD5-AS1* retards in vivo tumor growth of ESCC cells by reducing miR-383–SP1 axis output. (**A**) The volumes of tumor xenografts were measured for 1 month starting on day 10. The growth curve was plotted according to the time points and tumor volume data. *P < 0.05 vs the sh-NC group. (**B**) Representative images of tumor xenografts obtained from the sh-FGD5-AS1 group and sh-NC group. (**C**) At the end of the experiment, the tumor xenografts in the sh-FGD5-AS1 group and sh-NC group were excised and weighed. *P < 0.05 compared with the sh-NC group. (**D, E**) RT-qPCR was carried out to test *FGD5-AS1* and miR-383 expression in the tumor xenografts. *P < 0.05 vs the sh-NC group. (**F**) Western blotting was performed to determine the protein amount of SP1 in the tumor xenografts. *P < 0.05 vs the sh-NC group.

383–SP1 pathway may help to identify potential diagnostic and therapeutic targets in ESCC.

Conclusion

A knockdown of *FGD5-AS1* suppresses the malignant phenotype of ESCC cells both in vitro and in vivo by inhibiting miRNA sponging, thus increasing the binding of miR-383 to *SP1* mRNA. Therefore, this study validated the importance of the *FGD5-AS1*–miR-383–SP1 axis in ESCC tumorigenesis and offers a novel insight into the mechanism underlying the formation and progression of ESCC.

Ethics Approval and Informed Consent

The study protocol was approved by the Ethics Committee of Heze Municipal Hospital; the study was conducted in accordance with the principles of the Helsinki Declaration (approval number 150608). All subjects provided written informed consent prior to their enrollment in this study. The animal experimental protocols were approved by the Animal Care and Use Committee of Heze Municipal Hospital (approval number 150902). All experimental steps were in accordance with the Animal Protection Law of the People's Republic of China-2009 for experimental animals.

Data Sharing Statement

The datasets used and/or analyzed during the present study are available from the corresponding author on reasonable request.

Disclosure

The authors declare that they have no competing interests.

References

1. Cools-lartigue J, Spicer J, Ferri LE. Current status of management of malignant disease: current management of esophageal cancer. *J Gastrointestinal Surg*. 2015;19(5):964–972. doi:10.1007/s11605-014-2701-3
2. Torre LA, Bray F, Siegel RL, Ferlay J, Lortet-tieulent J, Jemal A. Global cancer statistics, 2012. *CA Cancer J Clin*. 2015;65(2):87–108. doi:10.3322/caac.21262

3. Arnold M, Soerjomataram I, Ferlay J, Forman D. Global incidence of oesophageal cancer by histological subtype in 2012. *Gut*. 2015;64(3):381–387. doi:10.1136/gutjnl-2014-308124
4. Smyth EC, Lagergren J, Fitzgerald RC, et al. Oesophageal cancer. *Nat Rev Dis Primers*. 2017;3(1):17048. doi:10.1038/nrdp.2017.48
5. Palladino-davis AG, Mendez BM, Fisichella PM, Davis CS. Dietary habits and esophageal cancer. *Dis Esophagus*. 2015;28(1):59–67. doi:10.1111/dote.2015.28.issue-1
6. Li B, Xu WW, Han L, et al. MicroRNA-377 suppresses initiation and progression of esophageal cancer by inhibiting CD133 and VEGF. *Oncogene*. 2017;36(28):3986–4000. doi:10.1038/onc.2017.29
7. Adelman K, Egan E. Non-coding RNA: more uses for genomic junk. *Nature*. 2017;543(7644):183–185. doi:10.1038/543183a
8. Duguang L, Jin H, Xiaowei Q, et al. The involvement of lncRNAs in the development and progression of pancreatic cancer. *Cancer Biol Ther*. 2017;18(12):927–936. doi:10.1080/15384047.2017.1385682
9. Thomson DW, Dinger ME. Endogenous microRNA sponges: evidence and controversy. *Nat Rev Genet*. 2016;17(5):272–283. doi:10.1038/nrg.2016.20
10. Geisler S, Coller J. RNA in unexpected places: long non-coding RNA functions in diverse cellular contexts. *Nat Rev Mol Cell Biol*. 2013;14(11):699–712. doi:10.1038/nrm3679
11. Dong P, Xiong Y, Yue J, et al. Exploring lncRNA-mediated regulatory networks in endometrial cancer cells and the tumor microenvironment: advances and challenges. *Cancers*. 2019;11(2):234. doi:10.3390/cancers11020234
12. Fang Y, Fullwood MJ. Roles, functions, and mechanisms of long non-coding RNAs in cancer. *Genomics Proteomics Bioinformatics*. 2016;14(1):42–54. doi:10.1016/j.gpb.2015.09.006
13. Gao H, Wang T, Zhang P, et al. Linc-ROR regulates apoptosis in esophageal squamous cell carcinoma via modulation of p53 ubiquitination by targeting miR-204-5p/MDM2. *J Cell Physiol*. 2020;235(3):2325–2335
14. Ma J, Xiao Y, Tian B, et al. Long noncoding RNA lnc-ABCA12-3 promotes cell migration, invasion, and proliferation by regulating fibronectin 1 in esophageal squamous cell carcinoma. *J Cell Biochem*. 2[illegible] (2):1374–1387.
15. Shi W, Wang Q, Bian Y, et al. Long noncoding RNA PA[illegible]DA promotes esophageal squamous carcinoma cell pr[illegible]y dissoc[illegible] ing from NF-YA but interact with SAFA. *Path[illegible] Res Pra*. 2019;2[illegible] (10):152604. doi:10.1016/j.prp.2019.15260[illegible]
16. Zhang C, Wang L, Yang J, et al. Micro[illegible]A-33[illegible]p sup[illegible]es esophageal squamous cell carcinom[illegible] progressi[illegible]via regulation of lncRNA DANCR and ZEB1. *Eu[illegible] Pharmacol*. [illegible]19;861:172590. doi:10.1016/j.ejphar.2019.1725[illegible]
17. Shen SN, Li K, Liu Y, Yang CL, He CY, [illegible]ng HR. Down-regulation of long noncoding RNA [illegible]VT1 inhibits es[illegible]hageal carcinoma cell migration and inv[illegible]ion and promotes [illegible]ell apoptosis via microRNA-145-m[illegible]ated inhi[illegible]ion of FSCN1. *Mol Oncol*. 2019;13(12):2554–2573. doi:[illegible]10[illegible]mol2.v13.12
18. Zhang Y, Mi[illegible]Y, Shang[illegible] et al. Li[illegible]NA-p21 leads to G1 arrest by p53 pathw[illegible]y in e[illegible]phageal [illegible]uam[illegible]s cell carcinoma. *Cancer Manag Res*. 2[illegible]9;11:620[illegible]6214. doi:[illegible]2147/CMAR.S197557
19. Li D[illegible]ang X[illegible] Cao G, Wang D, Chen Z. Long noncoding RNA P[illegible]AS1 promotes colorectal cancer cell proliferation, migration, [illegible] invasion through upregulating CDCA7 via sponging miR-302e. *In[illegible]tro Cell Dev Biol Anim*. 2019;55(8):577–585. doi:10.1007/s11626-019-00376-x
20. Lei Y, Shi Y, Duan J, et al. Identification of alternative splicing and lncRNA genes in pathogenesis of small cell lung cancer based on their RNA sequencing. *Adv Clin Exp Med*. 2019;28(8):1043–1050. doi:10.17219/acem/94392
21. Zhu H, Lu J, Zhao H, et al. Functional long noncoding RNAs (lncRNAs) in clear cell kidney carcinoma revealed by reconstruction and comprehensive analysis of the lncRNA-miRNA-mRNA regulatory network. *Med Sci Monit*. 2018;24:8250–8263. doi:10.12659/MSM.910773
22. Livak KJ, Schmittgen TD. Analysis of relative gene expression data using real-time quantitative PCR and the 2(-Delta Delta C(T)) method. *Methods*. 2001;25(4):402–408. doi:10.1006/meth.2001.1262
23. Xu G, Li N, Zhang Y, Zhang J, Xu R, Wu Y. MicroRNA-383-5p inhibits the progression of gastric carcinoma via targeting HDAC9 expression. *Braz J Med Biol Res*. 2019;52(8):e8341.
24. Azarbarzin S, Feizi MAH, Safaralizadeh R, Kazemzadeh M, Fateh A. The value of MiR-383, an intronic MiRNA, as a diagnostic and prognostic biomarker in intestinal-type gastric cancer. *Biochem Genet*. 2017;55(3):244–252. doi:10.1007/s10528-017-9793-x
25. Sui GQ, Fei D, Guo F, et al. MicroRNA-338-3p inhibits thyroid cancer progression through targeting AKT3. *Am J Cancer Res*. 2017;7(5):1177–1187.
26. Han RL, Wang FP, Zhang PA, Zhou XY, Li Y. miR-383 inhibits ovarian cancer cell proliferation, invasion and a[illegible]ic glycolysis by targeting LDHA. *Neoplasma*. 2017;64(2):244[illegible]52. doi:[illegible]4149/neo_2017_211
27. Wan P, Chi X, Du Q, et al. miR[illegible]383 promotes [illegible]olangiocarcinoma cell proliferation, migration, an[illegible]invasion throug[illegible] targeting IRF1. *J Cell Biochem*. 2018;119[illegible]2):9720[illegible]729. doi:10.[illegible]002/jcb.27286
28. Kashyap MK, Abdel-ra[illegible]han O. Expre[illegible]n, re[illegible]ation and targeting of receptor tyrosine[illegible]nases in [illegible]ophagea[illegible]amous cell carcinoma. *Mol Cancer*. 2018;[illegible]1):54. [illegible]:10.1186/s12943-018-0790-4
29. Testa U, Ca[illegible]i G, [illegible]i E. Eso[illegible]ageal cancer: genomic and molecular [illegible]aracterizati[illegible] stem [illegible]ell compartment and clonal evolutio[illegible] *M[illegible]icines*. 2017;[illegible]
30. Zong [illegible]Z, Fen[illegible]WT, Du N, Yu XJ, Yu WY. Upregulation of long noncoding RNA L[illegible]1-AS1 predicts a poor prognosis in patients with esop[illegible]ageal squamou[illegible]ll carcinoma. *Eur Rev Med Pharmacol Sci*. 2019;23(18):7929–7934. doi:10.26355/eurrev_201909_19007
31. He Z. LIN[illegible]0473/miR-497-5p regulates esophageal squamous cell carcinoma p[illegible]gression through targeting PRKAA1. *Cancer Biother Radiopharm*. 2019;34(10):650–659. doi:10.1089/cbr.2019.2875
32. Li [illegible]ng J, Luo X, et al. Overexpression of the long non-coding RNA FOXD2-AS1 promotes cisplatin resistance in esophageal squamous cell [illegible]inoma through the miR-195-Akt-mTOR axis. *Oncol Res*. 2019.
33. Chan JJ, Tay Y. Noncoding RNA:RNA regulatory networks in cancer. *Int J Mol Sci*. 2018;19(5):1310. doi:10.3390/ijms19051310
34. Chang WC, Hung JJ. Functional role of post-translational modifications of Sp1 in tumorigenesis. *J Biomed Sci*. 2012;19(1):94. doi:10.1186/1423-0127-19-94
35. Davie JR, He S, Li L, et al. Nuclear organization and chromatin dynamics–Sp1, Sp3 and histone deacetylases. *Adv Enzyme Regul*. 2008;48(1):189–208. doi:10.1016/j.advenzreg.2007.11.016
36. Bajpai R, Nagaraju GP. Specificity protein 1: its role in colorectal cancer progression and metastasis. *Crit Rev Oncol Hematol*. 2017;113:1–7. doi:10.1016/j.critrevonc.2017.02.024
37. Jiang W, Jin Z, Zhou F, Cui J, Wang L, Wang L. High co-expression of Sp1 and HER-2 is correlated with poor prognosis of gastric cancer patients. *Surg Oncol*. 2015;24(3):220–225. doi:10.1016/j.suronc.2015.05.004
38. Vizcaino C, Mansilla S, Portugal J. Sp1 transcription factor: a long-standing target in cancer chemotherapy. *Pharmacol Ther*. 2015;152:111–124. doi:10.1016/j.pharmthera.2015.05.008
39. Pan F, Mao H, Bu F, et al. Sp1-mediated transcriptional activation of miR-205 promotes radioresistance in esophageal squamous cell carcinoma. *Oncotarget*. 2017;8(4):5735–5752. doi:10.18632/oncotarget.13902
40. Xu H, Jiang J, Zhang J, Cheng L, Pan S, Li Y. MicroRNA-375 inhibits esophageal squamous cell carcinoma proliferation through direct targeting of SP1. *Exp Ther Med*. 2019;17(3):1509–1516. doi:10.3892/etm.2018.7106
41. Yang L, Sun K, Chu J, et al. Long non-coding RNA FTH1P3 regulated metastasis and invasion of esophageal squamous cell carcinoma through SP1/NF-kB pathway. *Biomed Pharmacother*. 2018;106:1570–1577. doi:10.1016/j.biopha.2018.07.129